Open Access Library Journal

Theoretical Study of the Interaction between Chitosan Constituents (Glucosamine and Acetylglucosamine Dimers) and Na^+ Ions

Marwa Emmanuel*, Alexander Pogrebnoi, Tatiana Pogrebnaya

Department of Materials, Energy Science and Engineering, The Nelson Mandela African Institution of Science and Technology, Arusha, Tanzania
Email: *marwaking39eti@gmail.com, *marwae@nm-aist.ac.tz

Received 10 October 2015; accepted 25 October 2015; published 30 October 2015

Abstract

The interaction of dimers of glucosamine and acetylglucosamine molecules with sodium ion has been studied using the DFT/B3LYP approach. The optimization of geometrical parameters and vibrational spectra calculations were done under 6-31G(d) basis set, and energies of the reactions were obtained using 6-311++G(d, p) basis set. The enthalpies of the association reactions of the dimers of glucosamine and acetylglucosamine with Na^+ have been determined. The internal hydrogen bonds OH…O and NH…O have been shown to play an important role in conformational behavior of a particular molecule.

Keywords

Chitosan, Glucosamine, Acetylglucosamine, Adduct, Geometrical Parameter, Vibrational Spectra, Enthalpies of Reactions, Thermodynamic Functions

Subject Areas: **Chemical Engineering & Technology**

1. Introduction

The functioning of any biological molecule depends fundamentally on the shape and flexibility, and further on interactions with neighboring environment, interactions provide feedback on their preferred structures and preferred bio-active conformer as well [1] [2]. For that reason several experimental and theoretical studies about interactions of different molecules have been done where different methods have been employed like nucleation, growth in liquid or gas phase to mention but a few [1]. Molecular structure and interactions lie in the area of molecular physics; it generally involves experimental methods like electronic and vibrational spectroscopy,

*Corresponding author.

How to cite this paper: Emmanuel, M., Pogrebnoi, A. and Pogrebnaya, T. (2015) Theoretical Study of the Interaction between Chitosan Constituents (Glucosamine and Acetylglucosamine Dimers) and Na^+ Ions. *Open Access Library Journal*, **2**: e1978. http://dx.doi.org/10.4236/oalib.1101978

mass spectrometry, and other techniques. The theoretical DFT calculations of electronic structure and force field can lead to structural assignment and more importantly, identify the interactions within the isolated molecules and between molecules and environment [3] [4]. An interesting feature and advantage of the DFT method is that it specifies the simplest structure which can demonstrate intricacies and challenges of larger and complex systems [5]. DFT provides theoretical scrutiny of the spectra to weigh against experiment, the structural view which they reflect, and the non-covalent interactions that control them [3] [6] [7].

Chitosan is a harmless and eco-friendly polysaccharide that has in recent times emerged as a promising contender for diverse applications [8] [9]. Different chitosan constituents conformers exist and they differ in the fractional content of acetylated units and the degree of polymerization [8] [10] [11]. Chitosan, a linear co-polymer of glucosamine and N-acetylglucosamine in a β1-4 linkage obtained by N-acetylation of chitin [11] [12], is a biodegradable polysaccharide with a wide range of biomedical applications such as sutures, wound dressing, bone substitutes, tissue engineering, and gene and drug delivery systems [3] [6] [10] [13]. It is a structural material that is nowadays commonly used in chemistry, medicine, and in various technologies [2] [6]. It is biocompatible, biodegradable, nontoxic, nonflammable, nonallergenic, antimicrobial, and inexpensive [2] [13]-[18]. The chitosan constituents, glucosamine and acetylglucosamine, play an important role in multifarious applications in different fields like pharmaceutics, cosmetics, biomedicine and agriculture to mention but a few.

Previous computation exertions had been done about interaction of chitosan constituents with heavy metals, alkali and halide ions [3] [19]. The present study is the continuation of our previous work [20] where two different conformers of glucosamine monomer named A_X and A_Y and acetylglucosamine B as well as their interaction with sodium ion were considered. Here we attempt to move a little further and investigate the interaction between dimers of glucosamine and acetylglucosamine (A_XA_X, A_YA_Y, and A_YB) with sodium ion. The aim of the this work is to determine the geometrical structure, vibrational spectra, and thermodynamic properties of the dimer molecules, A_XA_X, A_YA_Y, and A_YB, as well as their adducts with sodium ion, $A_XA_XNa^+$, $A_YA_YNa^+$, and A_YBNa^+, and the enthalpies of the association reactions between Na^+ and the dimers.

2. Computational Details

The DFT/B3LYP method under the 6-31G(d) basis set was applied for the calculations of the equilibrium geometrical parameters and vibrational spectra of dimers A_XA_X, A_YA_Y, A_YB and their complexes with Na^+. Embarking on this work an ensemble of low energy conformers of interest were generated using HyperChem program package [21]. Then the designed configurations were used in the optimization procedure with the Firefly software [22] partially based on the GAMESS (US) source code [23]. Vibrational spectra calculated proved the structures to be at equilibrium by the absence of imaginary frequencies. The energies of the reactions were computed with several basis sets from 6-31G(d) up to 6-311++G(d, p). For the visualization of the optimized structures, and specification of geometrical parameters and vibrational modes, the wxMacMolplot [24] and Chemcraft [25] softwares have been applied.

3. Results and Discussion

3.1. Geometrical Structure of Dimers and Adducts

The equilibrium structures of the A_XA_X, A_YA_Y, A_YB and adducts $A_XA_XNa^+$, $A_YA_YNa^+$, and A_YBNa^+ are shown in **Figure 1**, **Figure 2**. The selected geometrical parameters and atomic charges are given in **Table 1**, **Table 2**. The dimers and adducts comprise two rings, each of the ring made up of five carbon and one oxygen atom inserted between. These rings are fixed jointly by the glycosidic bond, the bond which ensures the stability and stiffness of this molecule [7] [10]. The glycosidic bond bends the rings in opposite direction extricating rings from each other and thus reduces repulsive forces flanked by the two.

A_XA_X and $A_XA_XNa^+$. In the A_XA_X dimer, glycosidic bond forms an angle C2-O12-C15 = 119˚ in **Figure 1(a)**, and **Table 1**, whose respective length C2-O12 and C15-O12 are 1.438 Å and 1.400 Å correspondingly. In the $A_XA_XNa^+$ complex the geometrical parameters are not changed drastically, the angle C2-O12-C15 is 118˚ the bond length C2-O12 is 1.426 Å and C15-O12 is 1.412 Å. That is the attachment of Na^+ to the dimer does not alter significantly the shape of the glycosidic bond and this is because Na^+ attaches at the distance far away from the bond. In the A_XA_X molecule hydroxyl group and amine group are in opposite sides to each other to reduce mutual repulsion of like charges. Amine groups are located in rather big distance between, 7.175 Å, thus the stable conformer of A_XA_X is formed. In the rings of A_XA_X the internal C-O-C groups exist, in the first ring

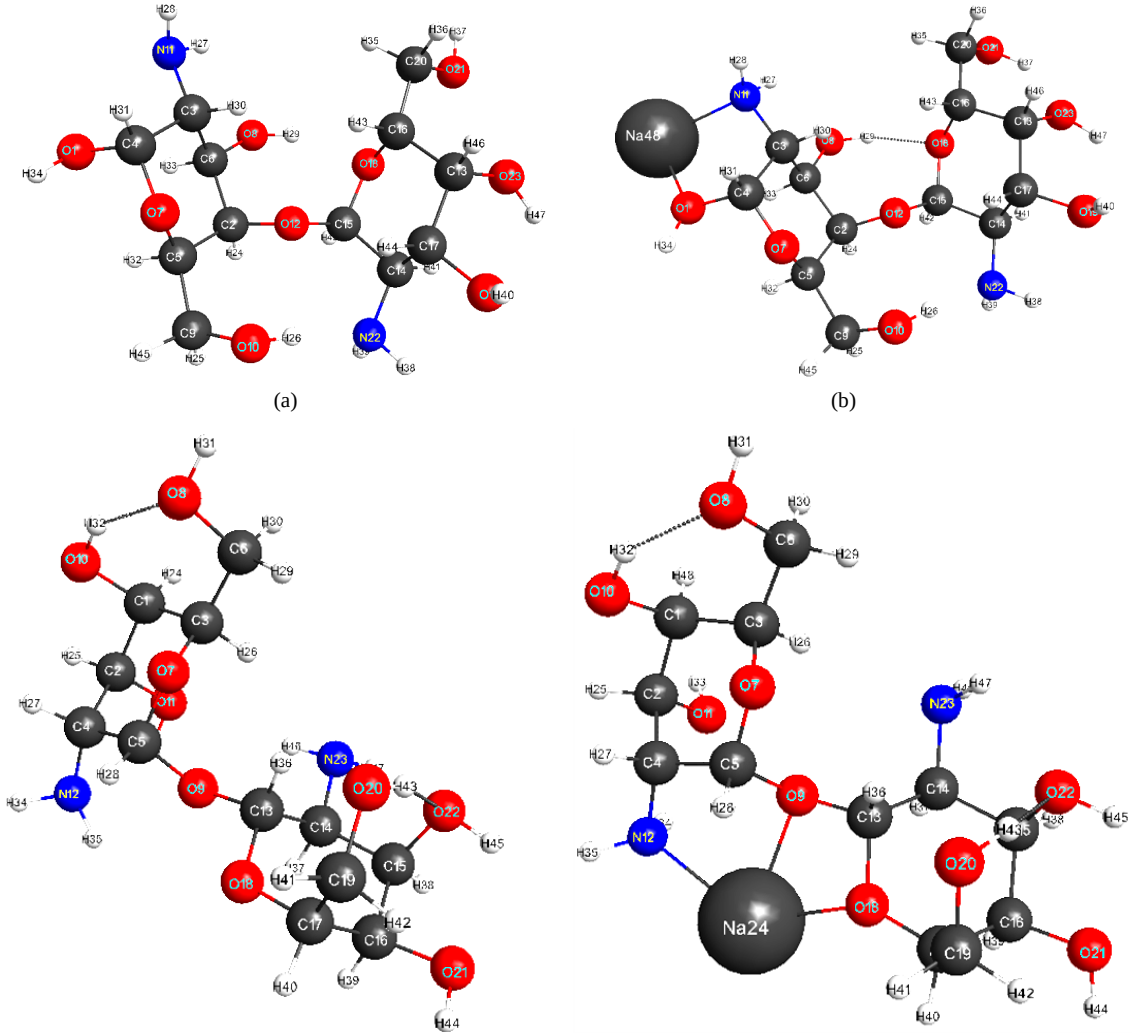

(a) (b)

(c) (d)

Figure 1. Equilibrium geometrical structure of the species: A_XA_X (a); $A_XA_XNa^+$ (b); A_YA_Y (c); $A_YA_YNa^+$ (d).

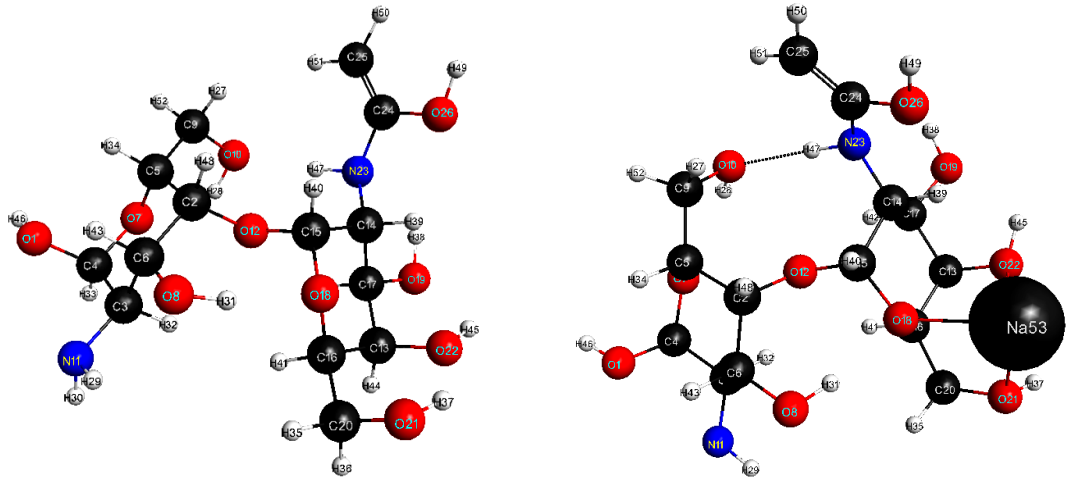

(a) (b)

Figure 2. Equilibrium geometrical structure of the species: A_YB (a) and A_YBNa^+ (b).

Table 1. Selected geometrical parameters and atomic charges of A_XA_X and $A_XA_XNa^+$.

Species	Internuclear distance R_e, Å		Valence angle, Deg		Torsion angle, Deg		Atom	Charge, a.u
A_XA_X	**O7-C5**	**1.433**	O1-C4-O7	112.0	O1-C4-O7-C5	61.5	**O1**	**–0.15**
	C4-O7	**1.419**	C4-O7-C5	**113.8**	C4-O7-C5-C2	60.3	**N11**	**–0.19**
	O10-C9	1.403	O10-C9-C5	117.3	O10-C9-C5-C2	64.5	**N22**	**–0.33**
	O12-C2	**1.438**	O12-C2-C6	111.8	O12-C2-C6-O8	59.5	O10	–0.28
	O8-C6	1.421	O8-C6-C3	112.2	O8-C6-C3-N11	56.6	O7	–0.02
	O1-C4	1.408	O1-C4-C3	109.2	O1-C4-C3-N11	53.8	O8	–0.17
	C15-O12	**1.400**	**C2-O12-C15**	**119.2**	C2-O12-C15-O18	100.2	O12	0.31
	C15-O18	**1.423**	**C15-O18-C16**	**114.3**	C15-O18-C16-C20	–174.1	O23	–0.10
	C16−O18	**1.439**					**C4**	**–0.64**
	O21-C20	1.412	O21-C20-C16	111.3	O21-C20-C16-C13	68.2	O19	–0.24
	O23-C13	1.411	O23-C13-C17	109.6	O23-C13-C17-O19	48.0		
	O19-C17	1.439	O19-C17-C4	150.5	O19-C17-C4-N22	–75.4		
$A_XA_XNa^+$	**O7-C5**	**1.448**	O1-C4-O7	111.3	O1-C4-O7-C5	69.2	**O1**	**–0.41**
	C4-O7	**1.382**	**C4-O7-C5**	**117.2**	C4-O7-C5-C2	53.8	**N11**	**–0.46**
	O10-C9	1.395	O10-C9-C5	115.8	O10-C9-C5-C2	67.0	**Na^+**	**0.83**
	O12-C2	**1.426**	O12-C2-C6	111.3	O12-C2-C6-O8	60.0	N22	–0.34
	O8-C6	1.412	O8-C6-C3	110.9	O8-C6-C3-N11	52.8	O10	–0.26
	O1-C4	1.460	O1-C4-C3	108.2	O1-C4-C3-N11	50.9	O7	0.03
	C15-O12	**1.412**	**C2-O12-C15**	**117.9**	C2-O12-C16-O18	125.1	O8	–0.15
	O18-C15	**1.417**	O18-C15-C14	111.5	O18-C15-C14-N22	178.3	O18	0.11
	C16-O18	**1.445**	**C15-O18-C16**	**115.9**	C15-O18-C16-C20	177.3	O21	–0.13
	O21-C20	1.402	O21-C20-C16	114.4	O21-C20-C16-C13	70.3	O23	–0.18
	O23-C13	1.421	O23-C13-C17	109.7	O23-C13-C17-O19	48.0	O19	–0.24
	Na^+-O1	2.227	O1-Na^+-N11	76.7	O1-Na^+-N11-C3	22.4	**C4**	**–0.58**
	Na^+-N11	2.335			C4-O1-Na^+-N11	3.5		
	O8-H29…O18	**1.853**						
A_YA_Y	**C5-O9**	**1.429**	**C5-O9-C13**	**117.4**	C5-O9-C13-O18	84.0	O7	0.13
	C13-O7	1.398					O9	0.09
	C3-O7	1.439	C3-O7-C5	115.2	C3-O7-C5-C4	–54.8	O10	–0.16
	C5-O7	1.400					O18	–0.01
	C13-O18	1.434	C13-O18-C17	114.8	C13-O18-C17-C16	–59.1	N12	–0.39
	C17-O18	1.428					N23	–0.30
	O10-H32…O8	1.865						
	O20-H43…O22	1.820						
$A_YA_YNa^+$	**C5-O9**	**1.453**	**C5-O9-C13**	**114.6**	C5-O9-C13-O18	103.3	O7	0.19
	C13-O7	1.406					O9	0.06
	C3-O7	1.446	C3-O7-C5	115.4	C3-O7-C5-C4	–53.2	O10	–0.12
	C5-O7	1.382					O18	–0.18
	C13-O18	**1.462**	**C13-O18-C17**	**116.7**	C13-O18-C17-C16	–59.7	N12	–0.49
	C17-O18	1.450	N12-Na^+-O18	129.2	N12-Na^+-O9-O18	162.3	N23	–0.19
	O10-H32…O8	1.853	N12-Na^+-O9	73.1			Na^+	0.83
	O20-H43…O22	1.864	O9-Na^+-O18	58.9				
	Na^+-O9	2.335						
	Na^+-O18	2.253						
	Na^+-N	2.347						

Table 2. Selected geometrical parameters and atomic charges of A_YB and A_YBNa^+.

Species	Internuclear distance, R_e, Å		Valence angle, Deg		Torsion angle, Deg		Atom	Charge, a.u
A_YB							O1	−0.37
	O1-C4	1.401	O1-C4-C3	109.7	O1-C4-C3-N11	55.0	O7	−0.42
	C4-O7	1.401	C4-O7-C5	109.7	C4-O7-C5-C9	55.0	O10	−0.42
	O10-C9	1.423	O10-C9-C5	113.2	O10-C9-C5-C2	75.2	N11	−0.44
	N11-C3	1.457	N11-C3-C6	109.2	N11-C3-C6-08	54.0	O12	−0.42
	C2-O12	**1.438**	**C2-O12-C15**	**118.3**	C2-O12-C15-O18	89.0	**O18**	**−0.42**
	C15-O18	1.423	C15-O18-C16	116.6	C15-O18-C16-C20	177.6	O19	−0.43
	C15-O12	**1.408**						
	O21-C20	1.406	O21-C20-C16	114.6	O21-C20-C16-C13	67.6	**O21**	**−0.40**
	O22-C13	1.425	O22-C13-C17	109.4	O22-C13-C17-O19	50.9	**O22**	**−0.45**
	O19-C17	1.421	O19-C17-C14	110.2	O19-C17-C14-N23	59.5	N23	−0.44
	O26-C24	1.369	O26-C24-N23	111.1	O26-C24-N23-C14	34.9	O26	−0.38
A_YBNa^+							**Na^+**	**0.74**
	O1-C4	1.394	O1-C4-C3	109.3	O1-C4-C3-N11	54.6	O1	−0.44
	O1-C4	1,394	O1-C4-O7	111.6	O1-C4-O7-C5	59.4	O7	−0.36
	C4-O7	1.435	C4-O7-C5	113.6	C4-O7-C5-C9	−171.2	O8	−0.43
	O10-C9	1.425	O10-C9-C5	113.3	O10-C9-C5-C2	74.4	O10	−0.47
	N11-C3	1.451	N11-C3-C6	109.0	N11-C3-C6-08	57.2	N11	−0.38
	C2-O12	**1.457**	**C2-O12-C15**	**119.2**	C2-O12-C15-O18	96.9	O12	−0.10
	N23-H47...O10	**1.930**						
	C15-O12	**1.378**						
	C15-O18	1.475	C15-O18-C16	113.1	C15-O18-C16-C20	−168.4	**O18**	**−0.40**
	O21-C20	1.440	O21-C20-C16	113.9	O21-C20-C16-C13	60.8	O19	−0.45
	O22-C13	1.444	O22-C13-C17	108.5	O22-C13-C17-O19	51.6	**O21**	**−0.49**
	O19-C17	1.417	O19-C17-C14	109.8	O19-C17-C14-N23	64.0	**O22**	**−0.61**
	O26-C24	1.373	O26-C24-N23	111.1	O26-C24-N23-C14	26.8	N23	−0.21
	Na^+-O18	2.351	O22-Na^+-O21	76.4	O22-Na^+-O21-C20	−68.1	O26	−0.50
	Na^+-O21	2.276	O22-Na^+-O18	76.0				
	Na^+-O22	2.312	O21-Na^+-O18	77.9				

C4-O7-C5 angle is 114˚, its respective bond lengths are C4-O7 = 1.419 Å and C5-O7 = 1.433 Å, in the other ring the C15-O18-C16 angle is the same and the bond lengths are 1.423 Å for C15-O18 and 1.439 Å for C16-O18. That is the internal C-O-C fragments are alike in both rings of A_XA_X implying to have the same chemical environment before Na^+ attachment.

In $A_XA_XNa^+$ adduct, the position of the Na^+ connection is ascribed to the negative charges of the N11, O1 and C4 (**Table 1**) and appropriate internuclear separations. The attachment of Na^+ creates two new bonds Na^+-O1 and Na^+-N11. Compared to A_XA_X, in $A_XA_XNa^+$ adduct the attached Na^+ results in some modification to the original structure, the C4-O7-C5 = 117˚ in the first ring whose respective bond lengths are C4-O7 = 1.382 Å and C5-O7 = 1.448Å, and the next ring C15-O18-C16 = 116˚ whose respective bond lengths are 1.417 Å for C15-O18 and 1.445 Å for C16-O18. Furthermore in the adduct $A_XA_XNa^+$, the internal hydrogen bond O8 - H29…O18 (1.853 Å) is formed which increases the adduct stability and stiffness.

A_YA_Y and $A_YA_YNa^+$. In the dimer A_YA_Y the amine groups are separated by distance of 4.979 Å that is significantly less as compared to A_XA_X (7.175 Å). This may lead to decrease in the stability of the dimer A_YA_Y because of the repulsive force experienced between amine groups. Also this dimer has two hydrogen bonds O10-H32…O8 and O20-H43…O22 whose respective lengths are 1.865 and 1.820 Å. The formation of these in-

ternal hydrogen bonds favors the stability of the dimer. In the glycosidic bond of A_YA_Y, the angle C5-O9-C13 is equal to 117˚ and the bond lengths C5-O9 and C13-O9 are 1.438 Å and 1.398 Å correspondingly (**Table 1**) while in the $A_YA_YNa^+$ complex, the similar angle C5-O9-C13 is 115˚ and the bond lengths are C5-O9 = 1.453 Å and C13-O9 = 1.406 Å. Thus akin to $A_XA_XNa^+$ the attachment of Na^+ to A_YA_Y does not bring essential change in the parameters of the glycosidic bond. At the same time contrary to $A_XA_XNa^+$, the position of Na^+ connection to A_YA_Y is close to the glycosidic bond; it attaches to two oxygen atoms (one of the glycosidic bond and another of the ring) and to the nitrogen atom connected with the second ring.

In $A_YA_YNa^+$ adduct, the position of the Na^+ attachment is credited to the negative charge −0.39 of the N12 in the dimer A_YA_Y and the appropriate internuclear separations and steric factors as well. Three new bonds are formed: Na^+-O9, Na^+-O18 and Na^+-N12 with internuclear separations 2.335 Å, 2.253 Å, and 2.347 Å, respectively. Two hydrogen bonds O10-H32…O8 and O20-H43…O22 remain in adduct $A_YA_YNa^+$, and their respective lengths do not change remarkably as compared to A_YA_Y.

A_YB and A_YBNa^+. The equilibrium structures of the A_YB complex and the A_YBNa^+ adduct are shown in **Figure 2**; and the selected geometrical parameters and atomic charges are given in **Table 2**. In the glycosidic bond of A_YB connecting two rings the angle C2-O12-C15 is equal to 118˚, and bond lengths are C2-O12 = 1.438 Å and O12-C15 = 1.408 Å. In the A_YBNa^+, the C2-O12-C18 angle is 119˚ and the respective bond lengths C2-O12 and O12-C15 are 1.457 Å and 1.378 Å, thus slight change in the C-O-C parameters are noticed when Na^+ is attached. In A_YBNa^+, three bonds are formed between Na^+ and negatively charged oxygen atoms O18, O21, O22. In A_YBNa^+ adduct the amino groups are located far apart at the distance of 7.244 Å between two nitrogen atoms to ebb electron-electron repulsion. Whereas in A_YB molecule there is no internal hydrogen bond, and in its adduct the hydrogen bond N23-H47…O10 is formed; this connotes that attachment of Na^+ stabilizes the species.

3.2. Vibration Spectra of Dimers and Adducts

In the calculated vibrational spectra there were no imaginary frequencies revealing the equilibrium geometrical structures of the species. The theoretical spectra of the dimer molecules and adducts with Na^+ ion are presented in **Figures 3-5**. The general feature of all these spectra is an existence of three regions of vibrational modes, which are approximately (i) below 1700 cm^{-1}, (ii) about 3000 cm^{-1}, and (iii) above 3300 cm^{-1}. The assignment of the most intensive peaks is considered below.

A_XA_X and $A_XA_XNa^+$. The vibrational spectra of A_XA_X and $A_XA_XNa^+$ adducts are shown in **Figure 3**. As is seen, majority of bands are located at a low frequency region 100 - 1690 cm^{-1} which correspond to O-H rocking, NH_2 scissoring, and ring bending vibrations. For the dimer A_XA_X the strongest peak seen at 1067 cm^{-1} is ascribed to bending of the first ring, and the subsequent peak at 1352 cm^{-1} is assigned to the bending of the second ring. An intricate vibration mode at 717 cm^{-1} relates to the bending of different fragments of the molecule. The middle region ranges from 2900 - 3100 cm^{-1} in both A_XA_X and $A_XA_XNa^+$ adduct; the most intensive peak relates to C-H stretching at about 3034 cm^{-1}. The higher frequency region ranges between 3400 - 3750 cm^{-1} for both A_XA_X and the $A_XA_XNa^+$ adduct where very intense O-H stretching modes are seen at about 3500 cm^{-1} and 3474 cm^{-1} for A_XA_X and $A_XA_XNa^+$, respectively. Also the peaks at 3581 cm^{-1} (A_XA_X) and 3444 cm^{-1} ($A_XA_XNa^+$) observed are assigned to the combination of O-H and N-H stretching modes.

A_YA_Y and $A_YA_YNa^+$. The vibrational spectra of A_YA_Y and $A_YA_YNa^+$ are shown in **Figure 4**. Majority of the vibrational bands manifests at the first frequency region. The most intensive vibrational peak is seen at 1089 cm^{-1} associated to bending of the ring, other peaks are seen also at 186 cm^{-1} relating to O-H rocking and ring bending, at 800 cm^{-1} NH_2 wagging, O-H rocking and a vibration band at ~1670 cm^{-1} assigned to the NH_2 scissoring. The similar bands are seen in $A_YA_YNa^+$ adduct. In the middle region at about 3000 cm^{-1} C-H stretching vibrational modes are seen for both A_YA_Y and $A_YA_YNa^+$ adduct; and in the higher frequency region O-H and NH_2 stretching vibrations may be observed between 3400 - 3750 cm^{-1} in both cases.

A_YB and A_YBNa^+. In the IR spectra of A_YB and A_YBNa^+ the most intensive bands are seen in low and high frequency regions (**Figure 5**). In the spectrum of A_YB molecule, the peak at 1741 cm^{-1} is assigned to a combination of C=C bond stretching and N-H rocking, the next band at 1035 cm^{-1} corresponds to the combination of C-O stretching and ring bending. Other peaks are ascribed to O-H rocking, N-H scissoring, and knotty vibration mode of the ring. In the middle region the C-H stretching vibration is observed at 3019 cm^{-1} for A_YB and at 3061 cm^{-1} for the adduct. Lastly in the third region, N-H, and O-H stretching vibration modes of the A_YB are

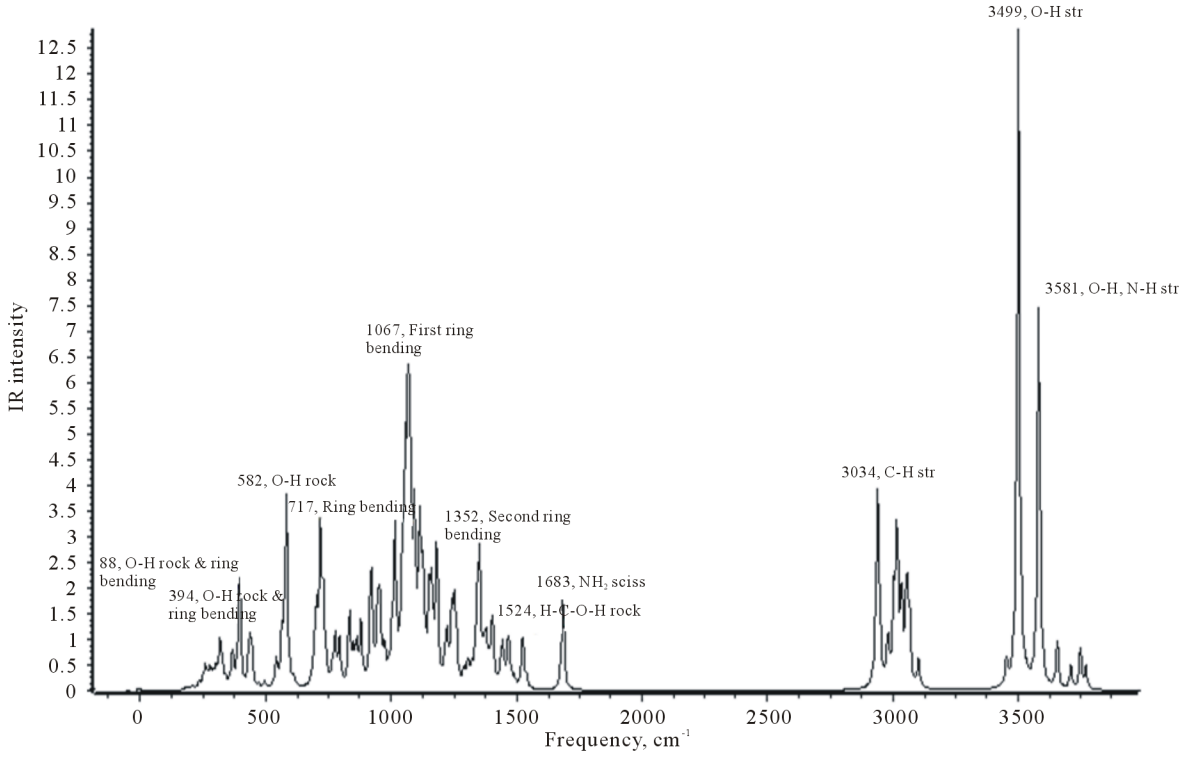

(a)

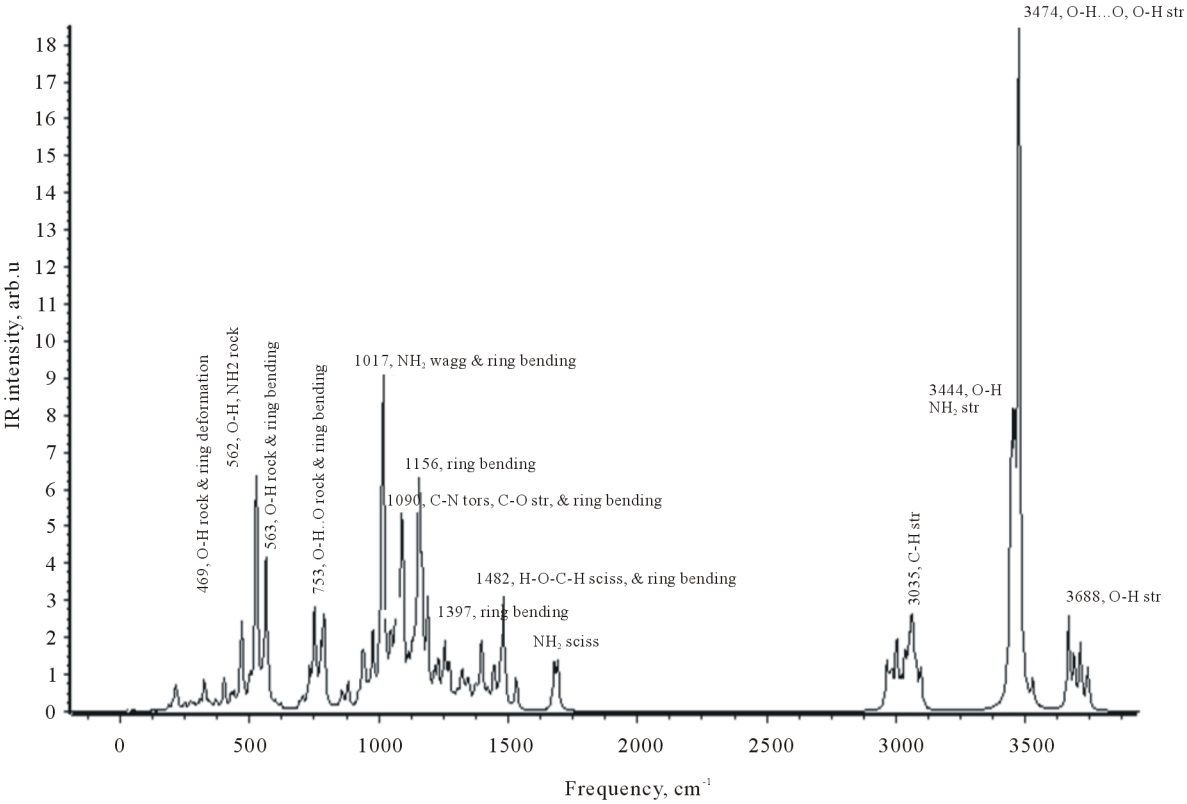

(b)

Figure 3. Theoretical IR spectra of A_XA_X (a) and $A_XA_XNa^+$ (b).

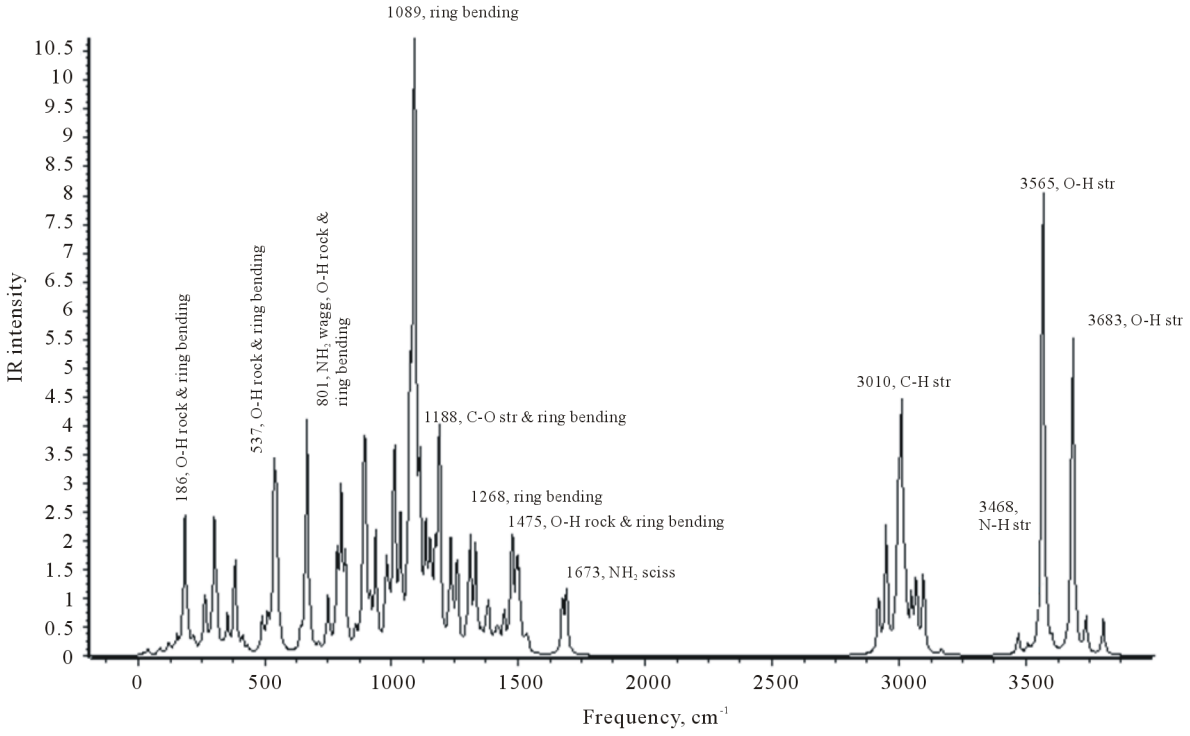

(a)

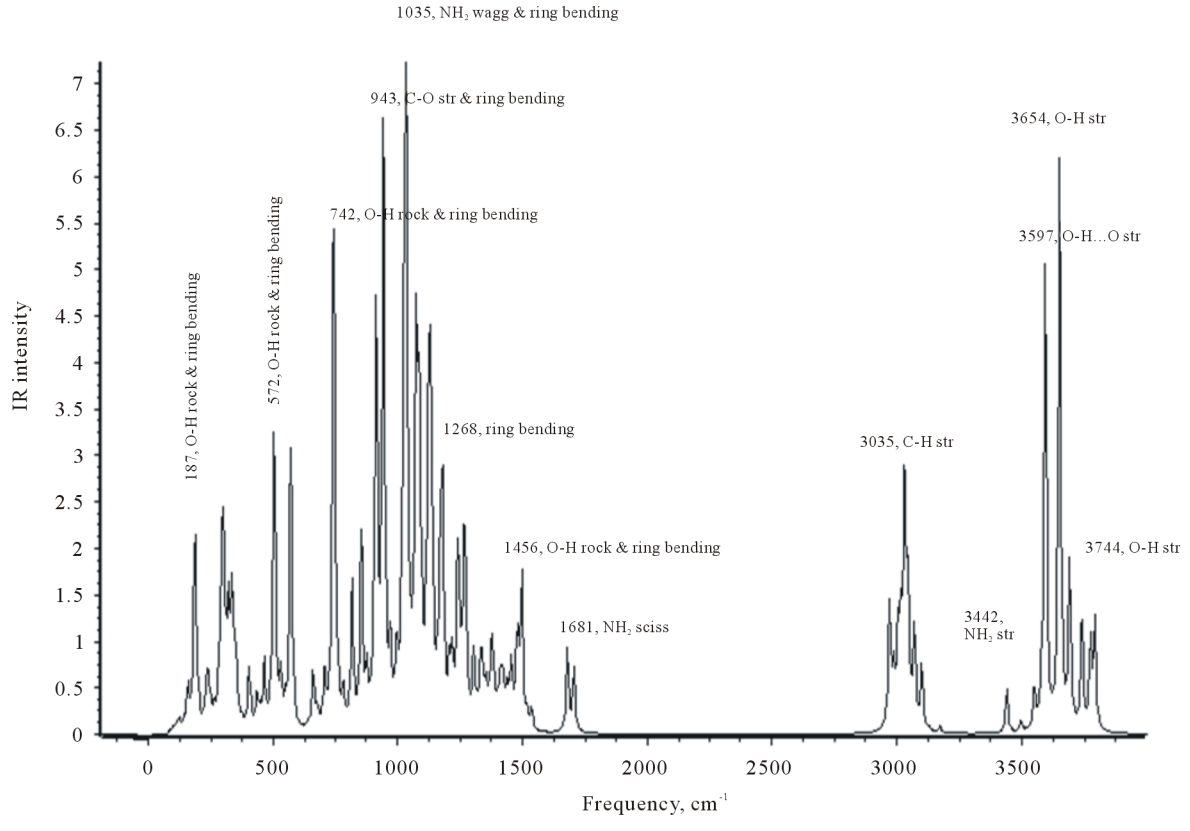

(b)

Figure 4. Theoretical IR spectra of A_YA_Y (a) and $A_YA_YNa^+$ (b).

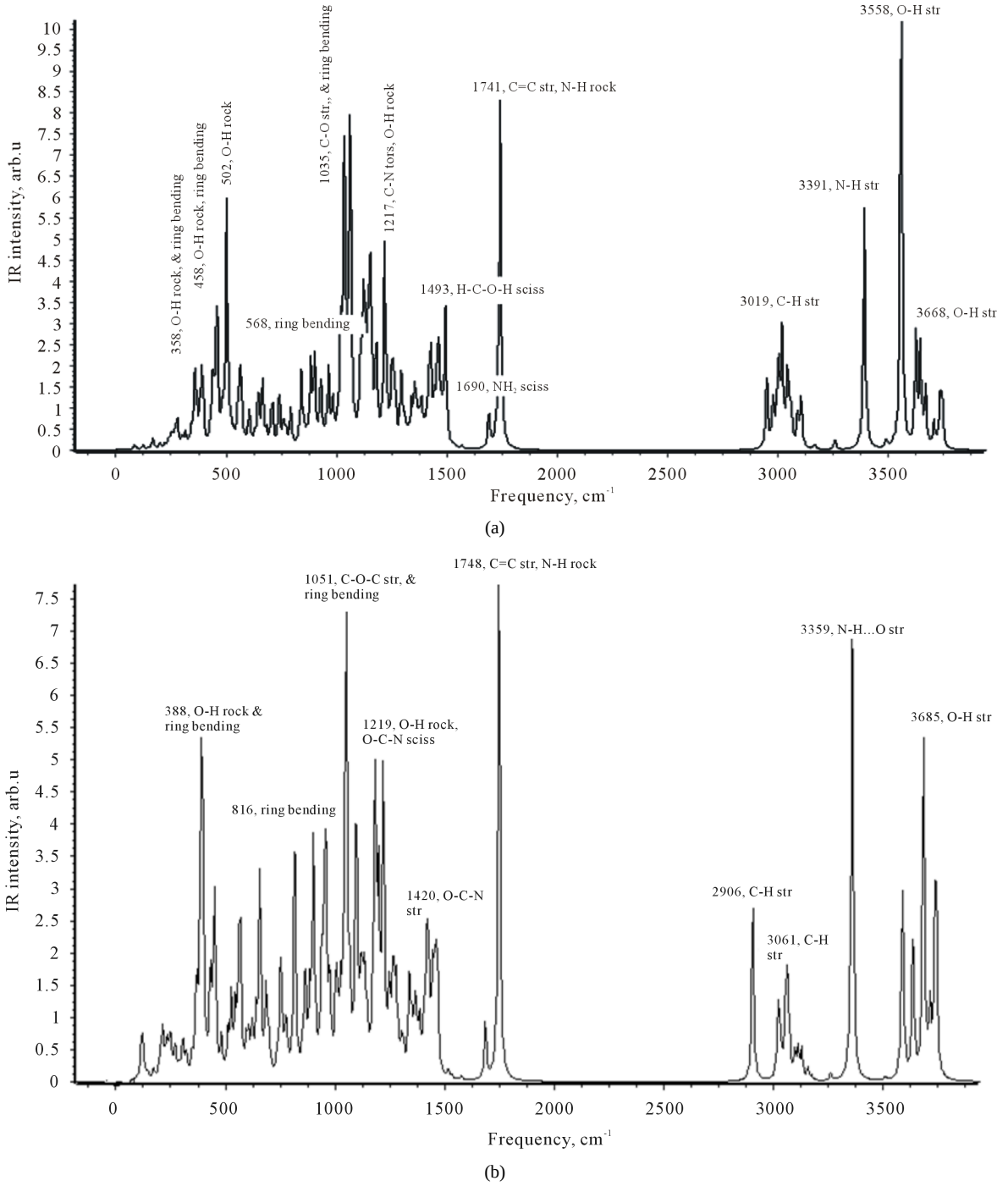

Figure 5. Theoretical IR spectra of A_YB (a), and A_YBNa^+ (b).

seen between 3391 - 3668 cm^{-1} while for A_YBNa^+ adduct the frequency 3359 cm^{-1} is assigned to the stretching vibration of NH…O (hydrogen bond).

Concluding this section on the spectra of the dimer molecules and the adducts with Na^+ ion, some similarities may be noted which are apparently due to the same functional groups of atoms, NH_2, CH, OH, COC, and other fragments, and the structural resemblance of the species as well. In the $AANa^+$, and $ABNa^+$ adducts, the Na^+ ion only participates in low frequency vibrations, less than 395 cm^{-1} of low IR intensity. Worth to mention here that the findings of this study are in accordance with the theoretical spectra of the glucosamine molecules A, AA,

and AAA [7], and ANa^+ and BNa^+ adducts [20] as well with the experimental IR spectra of chitosan [26] [27].

3.3. Thermodynamics of Association Reactions

The reactions of the sodium ion attachment to the dimer molecules were considered:

$$A_XA_X + Na^+ \rightarrow A_XA_XNa^+ \quad (1)$$

$$A_YA_Y + Na^+ \rightarrow A_YA_YNa^+ \quad (2)$$

$$A_YB + Na^+ \rightarrow A_YBNa^+ \quad (3)$$

The energies of the reactions Δ_rE were calculated as the difference between the total energies of the product and reactants:

$$\Delta_rE = E_{\text{prod}} - E_{\text{react}} \quad (4)$$

The enthalpies of the reactions $\Delta_rH°(0)$ were obtained using Δ_rE and the zero-point vibration energy corrections ΔZPVE:

$$\Delta_rH°(0) = \Delta_rE + \Delta\text{ZPVE} \quad (5)$$

$$\Delta\text{ZPVE} = \frac{1}{2}hc\left(\sum\omega_{i\ \text{prod}} - \sum\omega_{i\ \text{react}}\right) \quad (6)$$

where h is the Plank's constant, c is the speed of light in the free space, $\sum\omega_{i\ \text{prod}}$, and $\sum\omega_{i\ \text{react}}$ are the sums of the vibration frequencies of the product and reactants, respectively.

The enthalpies of the reactions (1)-(3) have been calculated under different basis sets, 6-31G(d), 6-31G(d, p), 6-311G(d), 6-311G(d, p), 6-31++G(d, p) and 6-311++G(d, p); the results are presented in **Figure 5**. For all three reactions, the similarity of the plots is observed. The general trend observed reveals the increase of the enthalpies of the reactions with the basis set extension. The difference between the lowest and highest values of $\Delta_rH°(0)$ for each reaction is about 50 kJ·mol^{-1}, thereafter the uncertainties for the enthalpies of the reactions may be estimated as half of this difference, that is ~25 kJ·mol^{-1}. The values energies Δ_rE, ΔZPVE, and enthalpies $\Delta_rH°(0)$ of the reactions obtained with the most extended basis set 6-311++G(d, p) are given in **Table 3**. The results indicate the association processes are highly exothermic, that implies a strong interaction between the cation and dimer molecules and high energetic stability of the corresponding adducts formed. The data obtained here are close to the enthalpies of attachment of sodium ion to monomer molecules, −196 kJ·mol^{-1} ($A_X + Na^+ = A_XNa^+$), −227 kJ·mol^{-1} ($A_Y + Na^+ = A_YNa^+$), and −229 kJ·mol^{-1} ($B + Na^+ = BNa^+$) [20]. Apparently likeness of these results relates to the similarity of the interacting moieties of the monomer or dimer molecules with Na^+ ion.

The Gibbs free energies $\Delta_rG°(T)$ of reactions (1)-(3) were calculated using the following equation:

$$\Delta_rG°(T) = \Delta_rH°(T) - T\Delta_rS°(T) \quad (7)$$

where $\Delta_rH°(T)$ is the enthalpy of the reaction at temperature T, $\Delta_rS°(T)$ is the change in entropy of the reaction. The thermodynamic functions of the A_XA_X, A_YA_Y, A_YB, $A_XA_XNa^+$, $A_YA_YNa^+$ and A_YBNa^+, have been computed using the OpenThermo software [28], those for Na^+ gaseous ions are taken from [29]. The geometrical parameters and vibrational frequencies needed for the thermodynamic functions calculations have been obtained under 6-31G(d) basis set. The thermodynamic functions of the species are given in **Table 4** for the temperature

Table 3. The reaction equations, energies Δ_rE, zero point vibrational energy corrections ΔZPVE and enthalpies $\Delta_rH°(0)$ of the reactions; in kJ·mol^{-1}.

N	Reaction	$-\Delta_rE$	ΔZPVE	$-\Delta_rH°$ (0 K)
1	$A_XA_X + Na^+ = A_XA_XNa^+$	245.0	9.9	235
2	$A_YA_Y + Na^+ = A_YA_YNa^+$	247.4	4.9	243
3	$A_YB + Na^+ = A_YBNa^+$	212.3	3.2	209

Table 4. Thermodynamic functions of A_XA_X, A_YA_Y, A_YB dimers and $A_XA_XNa^+$, $A_YA_YNa^+$ and A_YBNa^+ adducts.

	T, K	C_p^o, J·mol^{-1}·K^{-1}	$S°(T)$, J·mol^{-1}·K^{-1}	$H°(T) - H°(0)$, kJ·mol^{-1}	$\Phi°(T)$[a], J·mol^{-1}·K^{-1}
A_XA_X	298.15	384.91	671.75	63.53	458.68
	300	387.16	674.33	64.30	460.00
	400	495.93	800.83	108.53	529.50
	500	590.51	921.98	163.00	595.98
	600	668.09	1036.74	226.06	659.97
	700	731.26	1144.63	296.14	721.58
	800	783.35	1245.79	371.95	780.86
	900	826.97	1340.64	452.52	837.84
	1000	863.97	1429.74	537.12	892.62
$A_XA_XNa^+$	298.15	399.61	681.75	65.22	463.01
	300	401.77	684.23	65.96	464.36
	400	513.82	815.43	111.83	535.84
	500	610.35	940.79	168.19	604.40
	600	689.17	1059.29	233.31	670.44
	700	753.17	1170.50	305.53	734.02
	800	805.87	1274.62	383.57	795.16
	900	849.95	1372.16	466.42	853.91
	1000	887.36	1463.70	553.34	910.36
A_YA_Y	298.15	383.84	661.65	62.79	451.05
	300	385.93	664.03	63.50	452.36
	400	495.22	790.26	107.64	521.16
	500	590.01	911.27	162.05	587.17
	600	667.64	1025.95	225.07	650.84
	700	730.77	1133.78	295.09	712.22
	800	782.80	1234.86	370.85	771.29
	900	826.37	1329.65	451.37	828.12
	1000	863.35	1418.68	535.91	882.77
$A_YA_YNa^+$	298.15	408.10	690.29	67.24	464.77
	300	410.23	692.82	68.00	466.17
	400	520.53	826.21	114.63	539.64
	500	615.57	952.91	171.58	609.74
	600	693.14	1072.24	237.15	676.98
	650	726.21	1129.05	272.65	709.59
	700	756.09	1183.98	309.72	741.52
	800	807.92	1288.43	388.00	803.43
	900	851.25	1386.17	471.02	862.81
	1000	888.09	1477.81	558.04	919.77
A_YB	298.15	432.82	721.32	70.38	485.27
	300	435.19	724.01	71.18	486.73
	400	557.73	866.31	120.94	563.96
	500	662.62	1002.40	182.13	638.15
	600	747.97	1131.03	252.81	709.69
	700	817.16	1251.71	331.18	778.59
	800	874.08	1364.66	415.83	844.87
	900	921.69	1470.44	505.69	908.57
	1000	962.05	1569.69	599.93	969.76
A_YBNa^+	298.15	458.25	752.781	75.06	501.03
	300	460.65	755.62	75.91	502.60
	400	584.37	905.44	128.28	584.74
	500	689.48	1047.52	192.15	663.22
	600	774.64	1181.03	265.51	738.52
	700	843.49	1305.80	346.53	810.75
	750	873.10	1365.02	389.46	845.74
	800	900.05	1422.24	433.80	879.99
	900	947.32	1531.06	526.23	946.36
	1000	987.40	1633.00	623.02	1009.98

[a]$\Phi°(T) = -[H°(T) - H°(0) - TS°(T)]/T$ is the reduced Gibbs free energy.

range between 298 K and 1000 K. To find the enthalpies $\Delta_r H°(T)$, the enthalpy increments $H°(T) - H°(0)$ were used:

$$\Delta_r H°(T) = \Delta_r H°(0) + \Delta_r \left[H°(T) - H°(0) \right] \quad (8)$$

where the values of $\Delta_r H°(0)$ were obtained using Equation (5) and the values of $\Delta_r E$ calculated with 6-311++G(d, p) basis set.

The plot of the Gibbs free energies of reactions (1), (2) and (3) are presented in **Figure 6**. The values of $\Delta_r G°(T)$ are negative in a broad temperature range, this indicates that the attachment processes are spontaneous; $\Delta_r G°(T)$ become positive at temperatures higher than 1700 K for the reaction (1), and 2000 K for (2) and (3). For the reverse process it is evident that their corresponding adducts are stable with respect of the detachment of Na^+ ion in a broad temperature range (**Figure 7**).

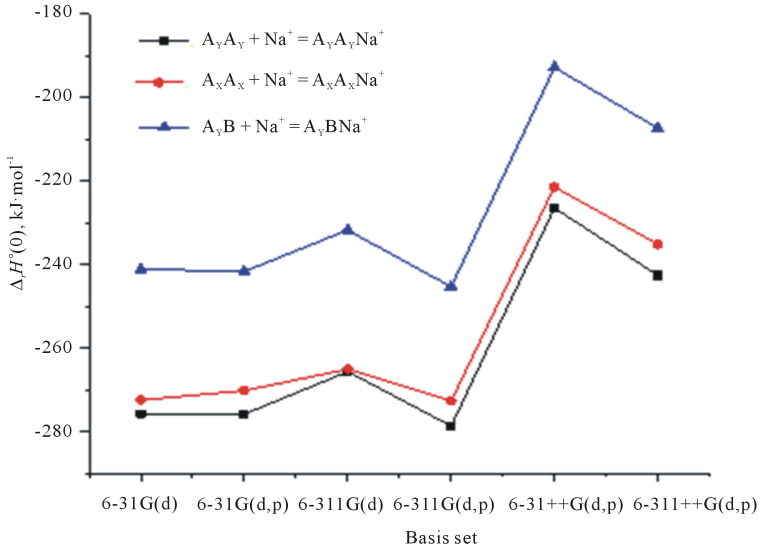

Figure 6. The calculated enthalpies of the reactions (1)-(3) vs. basis set.

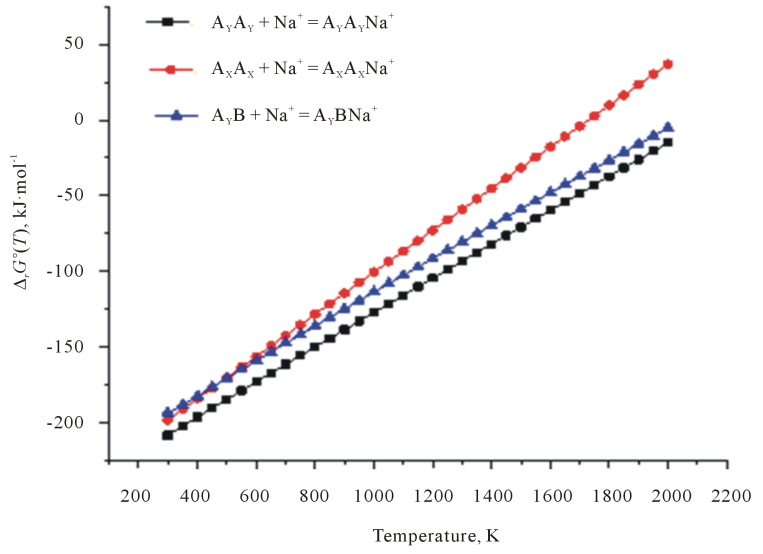

Figure 7. Gibbs free energy vs. temperature for the reactions $A_XA_X + Na^+ = A_XA_XNa^+$, $A_YA_Y + Na^+ = A_YA_YNa^+$ and $A_YB + Na^+ = A_YBNa^+$, 6-311++G(d, p) basis set.

4. Conclusions

The attachment of Na^+ ion to the dimers A_XA_X, A_YA_Y, A_YB to form adducts has been studied using the DFT/B3LYP method. The geometrical structures, vibrational spectra of the dimer molecules and their corresponding adducts due to Na^+ attachment have been determined. Position of Na^+ attachment is dictated by negative atomic charges occurrence, appropriate internuclear separations and steric factors. In the adducts $A_XA_XNa^+$ and $A_YA_YNa^+$, the sodium ion is linked to nitrogen and oxygen atoms; while in the A_YB molecule nitrogen atoms are screened by the acetyl groups, and therefore Na^+ sticks to three oxygen atoms instead.

The scrutiny of the calculated IR spectra revealed the general feature for all species, which is an existence of three regions composed of the similar vibrational bands which have been assigned to the certain functional groups of atoms, NH_2, CH, OH, COC, and other fragments. The structural resemblance of the species also has been brought to the similarity of the spectra. Thermodynamic characteristics of attachment have been determined. The exothermicity and spontaneity character of adducts formation have been ascertained.

Acknowledgements

The authors are grateful to The Nelson Mandela African Institution of Science and Technology, and The British Gas (BG group) for the sponsorship. In a special way we acknowledge a valuable assistance and service by the School of Computational and Communication Science and Engineering.

References

[1] Simons, J.P. (2009) Good Vibrations: Probing Biomolecular Structure and Interactions through Spectroscopy in the Gas Phase. *Molecular Physics*: *An International Journal at the Interface between Chemistry and Physics*, **107**, 2435-2458.

[2] Petrov, M., Lymperakis, L., Friák, M. and Neugebauer, J. (2012) *Ab Initio* Based Conformational Study of the Crystalline α-Chitin. *Biopolymers*, **99**, 22-34. http://dx.doi.org/10.1002/bip.22131

[3] Fattahi, A., Ghorat, M., Pourjavadi, A., Kurdtabar, M. and Torabi, A.A. (2008) DFT/B3LYP Study of Thermochemistry of D-Glucosamine, a Representative Polyfunctional Bioorganic Compound. *Scientia Iranica*, **15**, 422-429.

[4] Becke, A.D. (2014) Perspective: Fifty Years of Density-Functional Theory in Chemical Physics. *The Journal of Chemical Physics*, **140**, 18A301. http://dx.doi.org/10.1063/1.4869598

[5] Cohen, A.J., Mori-Sánchez, P. and Yang, W. (2011) Challenges for Density Functional Theory. *Chemical Reviews*, **112**, 289-320. http://dx.doi.org/10.1021/cr200107z

[6] Peña, I., Kolesniková, L., Cabezas, C., Bermúdez, C., Berdakin, M., Simão, A. and Alonso, J.L. (2014) The Shape of D-Glucosamine. *Physical Chemistry Chemical Physics*, **16**, 23244-23250. http://dx.doi.org/10.1039/C4CP03593C

[7] Onoka, I., Pogrebnoi, A. and Pogrebnaya, T. (2014) Geometrical Structure, Vibrational Spectra and Thermodynamic Properties of Chitosan Constituents by DFT Method. *International Journal of Materials Science and Applications*, 3, 121-128. http://dx.doi.org/10.11648/j.ijmsa.20140304.11

[8] Danielsen, S., Vårum, K.M. and Stokke, B.T. (2004) Structural Analysis of Chitosan Mediated DNA Condensation by AFM: Influence of Chitosan Molecular Parameters. *Biomacromolecules*, **5**, 928-936. http://dx.doi.org/10.1021/bm034502r

[9] Sionkowska, A., Wisniewski, M., Skopinska, J., Kennedy, C.J. and Wess, T.J. (2004) Molecular Interactions in Collagen and Chitosan Blends. *Biomaterials*, **25**, 795-801. http://dx.doi.org/10.1016/S0142-9612(03)00595-7

[10] Lehninger, A.L. (2004) Principles of Biochemistry. 4th Edition, W.H. Freeman, New York.

[11] Amaral, I.F., Granja, P.L. and Barbosa, M.A. (2005) Chemical Modification of Chitosan by Phosphorylation: An XPS, FT-IR and SEM Study. *Journal of Biomaterials Science*, *Polymer Edition*, **16**, 1575-1593. http://dx.doi.org/10.1163/156856205774576736

[12] Luo, Y.C. and Wang, Q. (2013) Recent Advances of Chitosan and Its Derivatives for Novel Applications in Food Science. *Journal of Food Processing and Beverages*, **1**, 13.

[13] Aranaz, I., Mengíbar, M., Harris, R., Paños, I., Miralles, B., Acosta, N., Galed, G. and Heras, Á. (2009) Functional Characterization of Chitin and Chitosan. *Current Chemical Biology*, **3**, 203-230.

[14] El-hefian, E.A., Nasef, M.M. and Yahaya, A.H. (2010) Preparation and Characterization of Chitosan/Polyvinyl Alcohol Blends—A Rheological Study. *E-Journal of Chemistry*, **7**, S349-S357. http://dx.doi.org/10.1155/2010/275135

[15] Benavente, M. (2008) Adsorption of Metallic Ions onto Chitosan: Equilibrium and Kinetic Studies. Licentiate Thesis, KTH, Stockholm.

[16] Tharun, J., Hwang, Y., Roshan, R., Ahn, S., Kathalikkattil, A.C. and Park, D.W. (2012) A Novel Approach of Utilizing Quaternized Chitosan as a Catalyst for the Eco-Friendly Cycloaddition of Epoxides with CO_2. *Catalysis Science & Technology*, **2**, 1674-1680. http://dx.doi.org/10.1039/c2cy20137b

[17] Prashanth, K.V.H. Advancement of Chitosan Based Nanoparticles for Present and Future Interests. Department of Meat, Fish and Poultry Technology CSIR-Central Food and Technological Research Institute, Mysore.

[18] Patrulea, V., Negrulescu, A., Mincea, M.M., Pitulice, L.D., Spiridon, O.B. and Ostafe, V. (2013) Optimization of the Removal of Copper (II) Ions from Aqueous Solution on Chitosan and Cross-Linked Chitosan Beads. *BioResources*, **8**, 1147-1165. http://dx.doi.org/10.15376/biores.8.1.1147-1165

[19] Terreux, R., Domard, M., Viton, C. and Domard, A. (2006) Interactions Study between the Copper II Ion and Constitutive Elements of Chitosan Structure by DFT Calculation. *Biomacromolecules*, **7**, 31-37. http://dx.doi.org/10.1021/bm0504126

[20] Emmanuel, M., Pogrebnoi, A. and Pogrebnaya, T. (2015) Interactions between Sodium Ion and Constituents of Chitosan: DFT Study. *International Journal of Materials Science and Applications*, **4**, 303-313.

[21] HyperChem$^{(TM)}$, H., Inc., 1115 NW 4th Street, Gainesville, Florida 32601, USA.

[22] Granovsky, A.A. (2014) Firefly Version 8.1.0. http://classic.chem.msu.su/gran/firefly/index.html

[23] Schmidt, M.W., Baldridge, K.K., Boatz, J.A., Elbert, S.T., Gordon, M.S., Jensen, J.H., Koseki, S., Matsunaga, N., Nguyen, K.A., Su, S., Windus, T.L., Dupuis, M. and Montgomery, J.A. (1993) General Atomic and Molecular Electronic Structure System. *Journal of Computational Chemistry*, **14**, 1347-1363. http://dx.doi.org/10.1002/jcc.540141112

[24] Bode, B.M. and Gordon, M.S. (1998) Macmolplt: A Graphical User Interface for GAMESS. Version 7.4.2. *Journal of Molecular Graphics and Modelling*, **16**, 133-138. http://dx.doi.org/10.1016/S1093-3263(99)00002-9

[25] Zhurko, G.A. and Zhurko, D.A. Chemcraft. Version 1.7 (Build 132). www.chemcraftprog.com

[26] Kunjachan, S., Jose, S. and Lammers, T. (2010) Understanding the Mechanism of Ionic Gelation for Synthesis of Chitosan Nanoparticles Using Qualitative Techniques. *Asian Journal of Pharmaceutics*, **4**, 148-153. http://www.asiapharmaceutics.info/text.asp?2010/4/2/148/68467 http://dx.doi.org/10.4103/0973-8398.68467

[27] Sobahi, T.R., Makki, M.S.I. and Abdelaal, M.Y. (2013) Carrier-Mediated Blends of Chitosan with Polyvinyl Chloride for Different Applications. *Journal of Saudi Chemical Society*, **17**, 245-250. http://dx.doi.org/10.1016/j.jscs.2011.03.015

[28] Tokarev, K. (2007-2009) OpenThermo. v.1.0 Beta 1 (C) ed. http://openthermo.software.informer.com

[29] Gurvich, L.V., Yungman, V.S., Bergman, G.A., Veitz, I.V., Gusarov, A.V., Iorish, V.S., Leonidov, V.Y., Medvedev, V.A., Belov, G.V., Aristova, N.M., Gorokhov, L.N., Dorofeeva, O.V., Ezhov, Y.S., Efimov, M.E., Krivosheya, N.S., Nazarenko, I.I., Osina, E.L., Ryabova, V.G., Tolmach, P.I., Chandamirova, N.E. and Shenyavskaya, E.A. (1992-2000) Thermodynamic Properties of Individual Substances. Ivtanthermo for Windows Database on Thermodynamic Properties of Individual Substances and Thermodynamic Modeling Software. Version 3.0. Glushko Thermocenter of RAS, Moscow.